Laboratory Investigation (2014) 94, 557–568

HIF-mediated metabolic switching in bladder outlet obstruction mitigates the relaxing effect of mitochondrial inhibition

Mari Ekman[1,2], Bengt Uvelius[3], Sebastian Albinsson[1] and Karl Swärd[1]

Prior work demonstrated increased levels of hypoxia-inducible factor-1α (HIF-1α) in the bladder following outlet obstruction, associated with bladder growth and fibrosis. Here we hypothesized that HIF induction in outlet obstruction also switches energetic support of contraction from mitochondrial respiration to glycolysis. To address this hypothesis, we created infravesical outlet obstruction in female Sprague–Dawley rats and examined HIF induction and transcriptional activation. HIF-1α increased after 6 weeks of outlet obstruction as assessed by western blotting and yet transcription factor-binding site analysis indicated HIF activation already at 10 days of obstruction. Accumulation HIF-2α and of Arnt2 proteins were found at 10 days, providing an explanation for the lack of correlation between HIF-1α protein and transcriptional activation. HIF signature targets, including *Slc2a1*, *Tpi1*, *Eno1* and *Ldha* increased in obstructed compared with sham-operated bladders. The autophagy markers Bnip3 and LC3B-II were also increased at 6 week of obstruction, but electron microscopy did not support mitophagy. Mitochondria were, however, remodeled with increased expression of Cox4 compared with other markers. In keeping with a switch toward glycolytic support of contraction, we found that relaxation by the mitochondrial inhibitor cyanide was reduced in obstructed bladders. This was mimicked by organ culture with the HIF-inducer dimethyloxalylglycine, which also upregulated expression of Ldha. On the basis of these findings, we conclude that HIF activation in outlet obstruction involves mechanisms beyond the accumulation of HIF-1α protein and that it results in a switch of the energetic support of contraction to anaerobic glycolysis. This metabolic adaptation encompasses increased expression of glucose transporters and glycolytic enzymes combined with mitochondrial remodeling. Together, these changes uphold contractility when mitochondrial respiration is limited.
Laboratory Investigation (2014) **94,** 557–568; doi:10.1038/labinvest.2014.48; published online 3 March 2014

KEYWORDS: Bnip3; Edn1; LC3-II; P4ha1; Slc2a3

Bladder outlet obstruction, such as seen in men with benign prostatic hyperplasia, is a prevalent clinical condition that leads to growth and remodeling of the urinary bladder. Prior work demonstrated increased levels of hypoxia-inducible factor-1α (HIF-1α) following bladder outlet obstruction.[1,2] Intravesical infusion of cobalt chloride, a known HIF inducer, moreover elicited bladder growth and angiogenesis similar to obstruction.[3] These findings indicate that HIF-1 has a role in remodeling and adaptation of the urinary bladder following outlet obstruction.

The HIF transcription factor complex is regulated by cellular O_2 tension such that one of the heterodimeric partners, the α-subunit, is hydroxylated and degraded in normoxia.[4–6] In hypoxia, the hydroxylation reaction slows down and α-subunits are stabilized, allowing for complex formation with HIF-1β (*Arnt*). The HIF complex binds to genomic hypoxia response elements and increases synthesis of proteins that promote angiogenesis and oxygen transport in blood.[7] HIF also redirects energy metabolism to allow for anaerobic energy production. Hypoxia-inducible, and HIF-driven, metabolic adaptation follows three general principles. First, the uptake and flux of glucose through glycolysis is increased by upregulation of glucose transporters (*Slc2a1* and *Slc2a3*) and glycolytic enzymes (*Tpi1*, *Eno1* and *Pgk1*).[5,8] Second, the product of glycolysis, pyruvate, is hindered from entering the citric acid cycle in mitochondria through upregulation of

[1]Department of Experimental Medical Science, Lund University, Biomedical Centre, BMC D12, Lund, Sweden; [2]Department of Biology, Faculty of Science, Sölvegatan 35, Lund, Sweden and [3]Department of Urology, Clinical Sciences, Lund University, Lund, Sweden
Correspondence: Dr K Swärd, PhD, Department of Experimental Medical Science, Lund University, Biomedical Centre, BMC D12, SE-221 84 Lund, Sweden.
E-mail: karl.sward@med.lu.se

Received 21 November 2013; revised 27 January 2014; accepted 10 February 2014

Pdk1, a kinase that inhibits formation of acetyl CoA, and through upregulation of *Ldha*, an enzyme that converts pyruvate to lactate.[5] The third principle for HIF-driven metabolic adaptation involves a reduced number of mitochondria through reciprocal changes in mitochondrial biogenesis and removal. HIF-1-mediated repression of mitochondrial biogenesis involves transcriptional upregulation of the c-Myc inhibitor *Mxi1* and a resultant reduction of *Ppargc1b* expression.[9] HIF-1-directed mitochondrial elimination, on the other hand, occurs through Bnip3-dependent mitophagy,[10] a process in which mitochondria are engulfed in autophagosomes and degraded.[11] This depends on binding of Bnip3 on the outer mitochondrial membrane to LC3B-II on the autophagosome, bridging the two membranes. In addition to its effect on mitochondrial mass, HIF may also remodel mitochondria to optimize the efficiency of respiration in oxygen-limited conditions through upregulation of cytochrome *c* oxidase 4-2.[12]

HIF-1α accumulation and binding to constitutively expressed HIF-1β represents the prototypical pathway for HIF-1-mediated transactivation. In certain cells and conditions,[13] HIF-2α may accumulate and dimerize with HIF-1β, but additional possibilities also exist. For example, HIF-1α may bind to HIF-2β (*Arnt2*) to form a functional HIF-1 complex that can rescue hypoxia-induced gene expression in HIF-1β-deficient cells.[14,15] HIF-2β is highly expressed in the kidney and in the hypothalamus where it is partly responsible for hypoxic induction of HIF-1 target genes.[16] Prior work demonstrated that HIF-2β mRNA is induced by bladder distension.[17] Provided that the HIF-2β protein changes in a similar manner, this may aid HIF-1 activation in the obstructed bladder. HIF-1α may also form transcription-competent dimers with Arntl2.[18] The dioxin receptor repressor Ahrr has finally been reported to inhibit HIF-dependent transcription.[19] Together, these possibilities add several layers of complexity to HIF activation that have not been addressed in bladder outlet obstruction.

Here we hypothesized that HIF activation results in metabolic adaptation after outlet obstruction.[20,21] This was tested by measuring HIF subunits in the bladder following outlet obstruction and by examining expression of glycolytic enzymes and of effectors of mitochondrial turnover. Our findings support the view that HIF-driven metabolic adaptation occurs in outlet obstruction and that this allows the bladder to cope with acute limitations in mitochondrial respiration. Our results moreover point to a complexity of HIF activation in outlet obstruction that goes beyond the accumulation of HIF-1α protein.

MATERIALS AND METHODS

Surgery

For surgical obstruction, rats (female, Sprague–Dawley, 200 g) were anesthetized with intramuscular injection of 100 mg/kg ketamine (Ketalar, Parke-Davis, Barcelona, Spain) and 15 mg/kg xylazin (Rompun: Bayer AG, Leverkusen, Germany). A midline abdominal incision was made and the urethra was freed by blunt dissection. A 1-mm stainless steel rod was aligned with the urethra and a tight ligature was placed around the rod and the urethra using 4/0 Prolene. The rod was removed and the ligature left *in situ* and the abdomen was closed with sutures in two layers. The experiment was terminated by killing the rats using gradually increasing CO_2 at 2, 4 and 10 days and at 6 weeks, respectively. Sham-operated rats went through the same procedure but without placement of the ligature. Each group consisted of 6–8 rats. In addition, for the microarray experiment we used a separate group of sham-operated rats and rats obstructed for 10 days and 6 weeks. One group of rats was first obstructed for 6 weeks and then re-operated to remove the obstruction. These were killed after another 10 days and are referred to as de-obstructed. A total of 6–8 rats were included in each group.

Microarray Analysis

The microarray experiment used here to assess HIF-1 activation was recently published by us[22] and is publicly available (GEO accession number GSE47080). Briefly, bladders from sham-operated rats, obstructed rats (10 days, 6 weeks) and de-obstructed rats were removed, cleaned and frozen in liquid N_2. Following RNA extraction, arrays for mRNAs and miRNAs were run as described.[22] We used transcription factor-binding site analysis to assess HIF activation. This method determines the enrichment of binding motifs in gene lists derived from microarray experiments by comparison with random samples of similar size from a promoter database.[23] The outcome is a probability to acquire the level of enrichment of motifs represented in the gene list by chance. We used the list of differentially expressed genes at 10 days of obstruction *vs* sham. The cutoff criteria applied were $q = 0$ (by significance analysis of microarrays) and either > 1.2-fold or < 0.8-fold change, respectively.

Western Blotting

Bladders were rapidly excised, cleaned and opened in Ca^{2+}-free HEPES-buffered Krebs solution (135.5 mM NaCl; 5.9 mM KCl; 1.2 mM $MgCl_2$; 11.6 mM glucose; 11.6 mM HEPES; pH 7.4 at 20 °C) and weighed. They were immediately frozen in liquid N_2 after gentle blotting on filter paper to remove excess buffer. Frozen bladders were then crushed in a stainless steel press that had been pre-cooled in liquid N_2. Before thawing, the resulting powder was dissolved in Laemmli sample buffer (62.5 mM Tris-HCl; 5% (w/v) SDS; 10% glycerol; 0.02% bromophenol blue). After protein determination using the DC™ protein assay (Bio-Rad), mercaptoethanol was added to a final concentration of 5%. Protease inhibitor cocktail (P 8340, Sigma Aldrich) and phosphatase inhibitor cocktail (#1862495, Thermo Scientific) were added. As we experienced conversion of the HIF-1α immunoreactive band at 120 kDa to an 80 kDa species with multiple freeze–thaw cycles, we prepared small (50 μl) lysate aliquots that were maintained at −80 °C and thawed only

once. In all, 20 μg of protein was loaded per lane on Criterion precast gels (any kD or 4–15%) with 18 wells (Midi, Bio-Rad). Kaleidoscope Precision Plus molecular weight markers were loaded in the outer lanes. Semi-dry transfer to 0.2 μm nitrocellulose was done using the Trans-Blot Turbo transfer system (Bio-Rad) at the high molecular weight setting. Proteins remaining on the gels after transfer were stained using Bio-Safe Coomassie (Bio-Rad). Membranes were blocked in 1% Tris-buffered saline casein blocker (Bio-Rad) for 2 h and subsequently incubated overnight with primary antibody diluted in the same solution.

The following primary antibodies were used: HIF-1α (Hif1a, H1alpha67, Abcam, 1:200; NB100-479, Novus Biologicals, 1:500), HIF-2α (Epas1, PA1-16510, Thermo Scientific, 1:200), Arnt2 (sc-5581, Santa Cruz, 1:200), Glut-1 (Slc2a1, 07-1401, EMD Millipore, 1:500), Glut-3 (Slc2a3, sc-30107, 1:200), Enolase-1 (Eno1, ab155102, Abcam, 1:1000), triosephosphate isomerase (Tpi1, ab28760, Abcam, 1:10 000), phosphoglycerate kinase 1 (Pgk1, LS-B5809, LifeSpan Biosciences, 1:2000), lactate dehydrogenase A (Ldha, #2012, Cell Signaling, 1:1000), lysyl oxidase (Lox, ABT112, EMD Millipore, 1:2000), endothelin 1 (Edn1, ab2786, Abcam, 1:500), prolyl 4-hydroxylase α_1 (P4ha1, GTX89145, GeneTex, 1:1000), c-Met (Met, sc-8057, Santa Cruz Biotechnology, 1:200), pim-1 oncogene (Pim1, #3247, Cell Signaling, 1:1000), Bnip3 (#3769, Cell Signaling, 1:1000), LC3B (Map1lc3b, ab48394, Abcam 1:500), sulfite oxidase (Suox, ab129094, Abcam, 1:5000), NADH dehydrogenase (ubiquinone) complex I assembly factor 1 (Ndufaf1, ab79826, Abcam, 1:5000), citrate synthase (Cs, Abcam, ab96600, 1:500), cytochrome *c* oxidase subunit IV (Cox4, #4844, Cell Signaling, 1:1000), transcription factor A, mitochondrial (Tfam, GTX59889, GeneTex, 1:1000), HSP90 (610418, BD Transduction Laboratories, 1:1000), β-actin (Actb, A5441, Sigma, 1:1000) and caveolin-1 (Cav1, D46G3, Cell Signaling, 1:1000).

Immunofluorescence

Bladder halves, cut in the rostro-caudal direction, were immersed in phosphate-buffered saline (PBS) containing 4% paraformaldehyde and maintained in this solution at room temperature overnight. They were then rinsed in PBS (× 3), mounted in OCT compound in Tissue-Tek cryomolds and frozen on dry ice. In all, 10 μm sections were cut in a cryostat and frozen. For staining, sections were rinsed (× 3, PBS) and incubated with primary antibody overnight (diluted in PBS with 5% bovine serum albumin and 1% Triton X-100). After three washes and incubation with secondary antibody (Molecular Probes, Eugene, OR, USA, diluted 1:500 in PBS with 5% bovine serum albumin and 1% Triton X-100, 2 h) sections were incubated for 5 min with bisbenzimide (1 μg/ml in PBS) to stain DNA. Following further washes (× 3, PBS) and mounting in 50% glycerol, fluorescence micrographs were captured using a Zeiss LSM 510 confocal microscope and a 63 × objective. The antibodies used were Glut-1 (a.k.a. Slc2a1, 07-1401, EMD Millipore, 1:100), Edn1 (ab2786, Abcam, 1:100) and caveolin-1 (610407, BD Transduction Laboratories, 1:100; D46G3, Cell Signaling, 1:1200).

Electron Microscopy

Three control and three 6 week-obstructed rats were used. After carbon dioxide asphyxiation as above the abdomen was opened, the urethra and the ureters were ligated, and the bladders were dissected out and transferred to 2.5% glutaraldehyde in 150 mM sodium cacodylate buffer (pH 7.4). After 30 min, the bladders were cut open longitudinally, emptied and then transferred to new fixative. After 2 h, mid-ventral segments were dissected and transferred to PBS. The specimens were post-fixed in 1% osmium tetroxide for 2 h, block-stained with uranyl acetate, dehydrated and embedded in Araldite. Semithin sections were cut and stained with toluidine blue and examined in a light microscope. Areas with cross-sectioned muscle bundles were chosen and cut for electron microscopy. The sections were grid stained with lead citrate and examined in a JEOL JEM 1230 electron microscope. Morphometry was performed using ImageJ (NIH, Bethesda, MD, USA). The number of mitochondria per unit cross-sectioned cell area was measured on at least 16 digital photos per bladder corresponding to at least 246 μm^2 (magnification 25k). Diameter of cross-sectioned mitochondria was determined using 80k digital photos. Thirty mitochondrial diameters were measured for each bladder. Relative cell area occupied by mitochondria was calculated from their mean diameter and their number per unit cell area.

Contractility

Rat bladder strips without mucosa were secured at both ends to stainless steel pins in 4-channel myographs (610 M; Danish MyoTechnology, Aarhus, Denmark) using 6/0 silk (Vömel, Germany). The myograph baths were filled with aerated HEPES-buffered Krebs solution (composition as above but also containing 2.5 mM $CaCl_2$ and pH 7.4 at 37 °C) and a basal tension of 8 mN was applied. Force was digitized using an AD Instruments AD-converter and recorded in LabChart7. After equilibration, strips were contracted repeatedly with 60 mM K^+ (obtained by replacing NaCl with KCl) until two consecutive contractions were equally forceful. In all, 3 mM cyanide was added from a stock solution after 7 min of contraction. Relaxation was assessed by averaging the force trace over the next 7 min and normalization was versus force just before addition of cyanide.

Organ Culture

To examine whether the metabolic adaptation seen in outlet obstruction is mimicked by the known HIF-inducer dimethyloxalylglycine (DMOG), rat detrusor strips were prepared and organ cultured with 300 μM DMOG at 37 °C and 5% CO_2/air in a humidified incubator. Strips without mucosa were maintained in DMEM/Ham's F12 medium (Biochrom, FG4815) supplemented with 50 U/ml penicillin and 50 μg/ml

streptomycin (Biochrom, A2213) as described.[24] Strips were harvested for biochemical and mechanical experiments after 5 days of culture.

Statistical Analysis

For microarray data, we used significance analysis of microarrays (SAM). This returns a *q*-value that is an equivalent of false discovery rate. $q = 0$ was considered significant, and is denoted by * in the figures reporting mRNA data. Significance testing was done on log-transformed expression data throughout, using one-way ANOVA followed by either Dunnett's multiple comparison test or Bonferronis's multiple comparisons test. Correlations were tested using linear regression analysis. Comparisons between two groups were done using Student's *t*-test. All analyses except the SAM analysis were done in GraphPad Prism (5.02).

RESULTS

HIF-1α Protein Increases after Outlet Obstruction

We surveyed the relative expression of *Hif1a*, *Epas1* (HIF-2α) and *Hif3a* mRNA in control and obstructed bladders using microarrays (GEO accession number GSE47080).[22] The mRNA level for *Hif1a* exceeded that of *Epas1* (Figure 1a), and *Hif3a* was undetectable. A modest, but not quite significant ($q = 0.03$, $P = 0.001$, $n = 6$), increase of *Hif1a* mRNA was seen in obstructed (10 days) compared with sham-operated rats. We therefore first focused on *Hif1a* and measured its protein level (Figure 1b, top blot) in whole bladder lysates from sham-operated and obstructed (2 days, 4 days, 10 days and 6 weeks) rats. A major species at 120 kDa, the expected molecular weight of HIF-1α, increased after 6 weeks of outlet obstruction (Figure 1b, summarized data in c). Another antibody against HIF-1α similarly demonstrated that an intense band migrating at 120 kDa was unchanged throughout 10 days, but increased at 6 weeks (data not shown). This supported the view that HIF-1α protein increases in the bladder following chronic outlet obstruction.

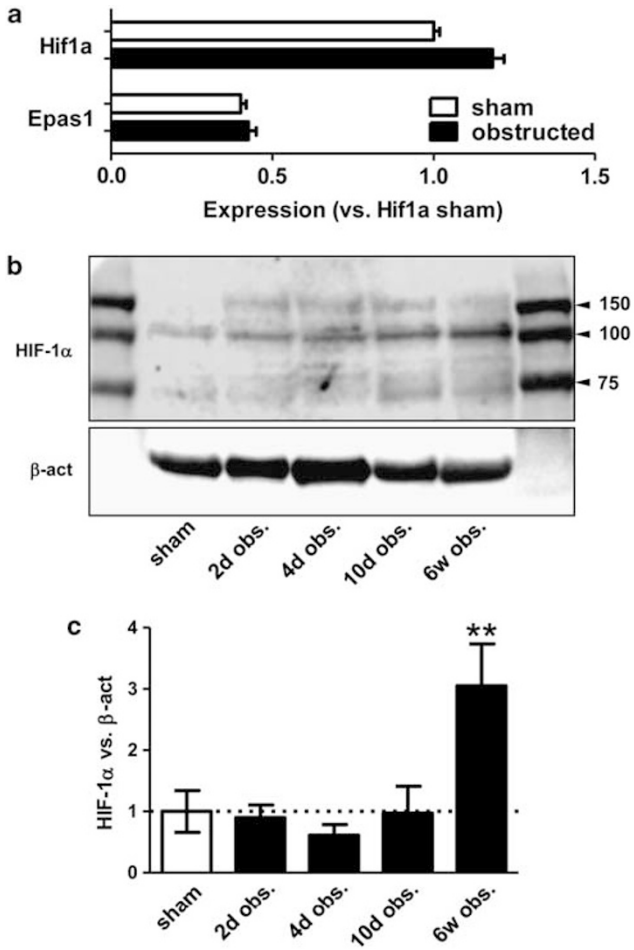

Figure 1 HIF-1α protein accumulates in the rat bladder following outlet obstruction. Panel **a** shows mRNA levels for *Hif1a* (HIF-1α) and *Epas1* (Hif-2α) in sham-operated and obstructed (10 days) bladders. Data are from a microarray experiment and normalization is against *Hif1a* in bladders from sham-operated controls. Panel **b** shows western blots for HIF-1α and β-actin, respectively. The membrane was cut above the 50 kDa marker and the upper half was incubated with HIF-1α antibody whereas the lower half was incubated with a β-actin antibody. The molecular weights of the markers are indicated to the right. Summarized data from six independent experiments are shown in panel **c**. HIF-1α was first normalized to β-actin and then to the mean HIF-1α/β-actin ratio for the sham-operated controls. **Indicates $P < 0.01$ *vs* sham.

Confirmation of HIF Activation after Outlet Obstruction by Transcription Factor-Binding Site Analysis

To further support HIF activation, we tested its transcriptional impact. For this, we used a gene set comprising differentially expressed genes after obstruction (10 days) compared with sham (GEO accession number GSE47080).[22] We compared the prevalence of HIF motifs to that of repeated random draws of identical size from a promoter database. This demonstrated significant enrichment of HIF-binding sites ($P = 0.00028$). To illustrate the apparent discrepancy between HIF-1α accumulation, occurring at 6 weeks, and HIF-mediated transcriptional activation, occurring already at 10 days, we examined if the protein level of HIF-1α correlated with the mRNA levels for established HIF targets (Supplementary Figure 1 shows time courses for 11 HIF target mRNAs). No significant correlation with HIF-1α protein were found for the HIF target *Slc2a1* (Glut1, Figure 2a), or indeed any of the 11 target mRNAs in Supplementary Figure 1 (correlations not shown).

Accumulation of HIF-2α and Arnt2 in Outlet Obstruction

In an effort to understand how HIF can have an apparent transcriptional impact in the absence of HIF-1α protein accumulation at 10 days of obstruction, we first examined induction of HIF-2α. This protein accumulated earlier than HIF-1α (Figure 2b) and a significant increase was seen at 10 days. We also surveyed the microarrays for binding partners for the α-subunits and found significant accumulation of *Arnt2* and *Arntl2* as well as repression of *Ahrr* (Figure 2c). Using western

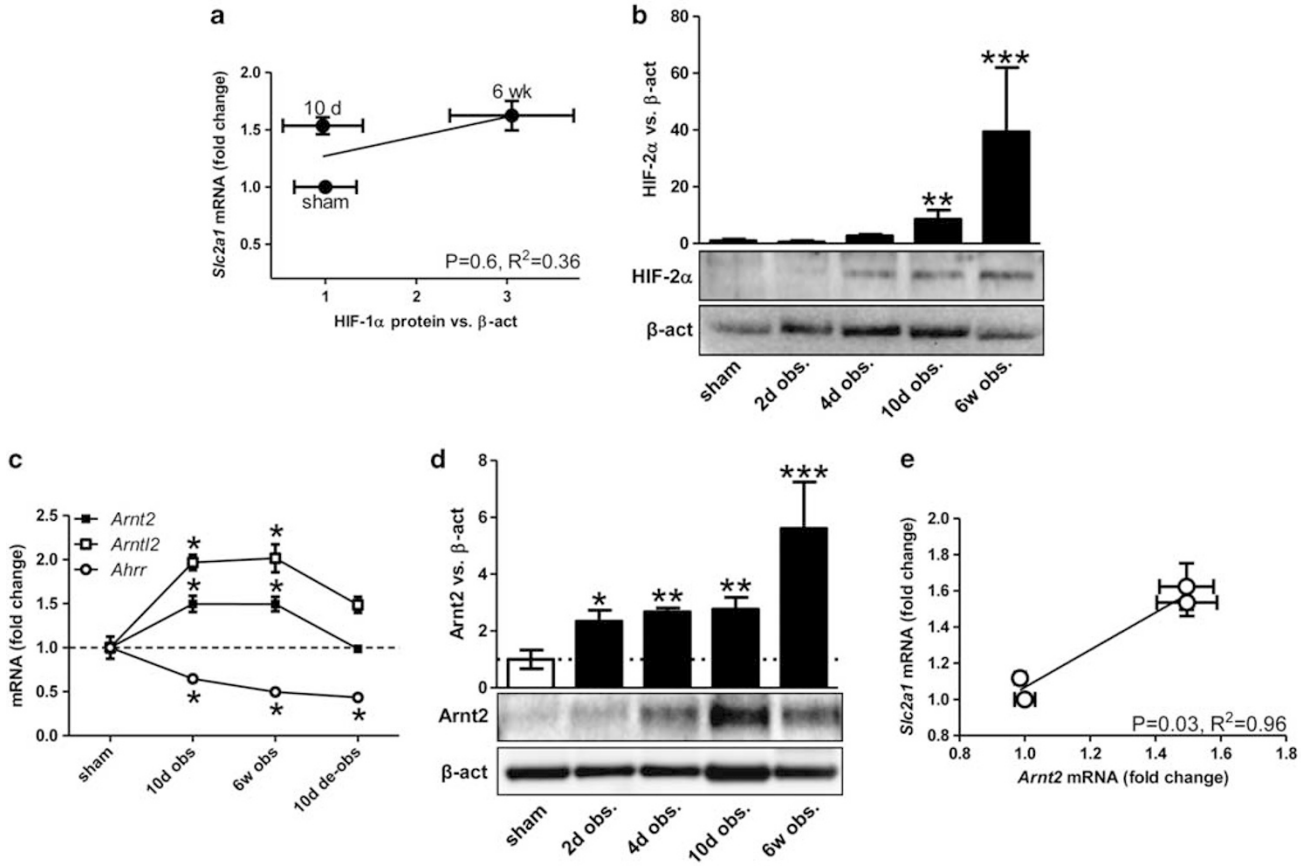

Figure 2 HIF-1 target mRNAs increase before the HIF-1α protein and this may be explained by reciprocal changes in HIF-β-subunits and Ahrr. No significant correlation was seen between HIF-1α protein and *Slc2a1* (Glut-1, panel **a**) mRNA. The different time points are indicated near the respective symbols. Similar results were obtained for 11 distinct HIF targets (data not shown). Panel **b** shows induction of HIF-2α in outlet obstruction. Typical blots for HIF-2α and β-actin are shown below the bar graph. Panel **c** shows mRNA levels for *Arnt2* (HIF-2β), *Arntl2* (a.k.a. Bmal2 and MOP9) and *Ahrr* in sham-operated control bladders, after 10 days and 6 weeks of obstruction and after de-obstruction, respectively. The data in **c** are from our recent microarray experiment.[22] Panel **d** shows Arnt2 protein in sham-operated control bladders and after different times of obstruction ($n=6$). Panel **e** shows correlation between *Arnt2* and *Slc2a1* mRNAs. In panels **b** and **d** *, **, and *** denote $P<0.05$, $P<0.01$ and $P<0.001$, respectively. In panel **c** * denotes $q=0$.

blotting, we found evidence for accumulation of Arnt2 (HIF-2β) well before 10 days of obstruction (Figure 2d). These changes may help explain HIF activation in the absence of HIF-1α accumulation at 10 days of obstruction. In keeping with this possibility, a significant correlation was seen for *Arnt2* and *Slc2a1* mRNAs (Figure 2e).

Glycolytic Enzymes, Ldha and Glucose Transporters Increase after Outlet Obstruction

Figure 3a shows upregulation of HIF signature target mRNAs encoding glycolytic enzymes (*Tpi1*, *Pgk1* and *Eno1*) and glucose transporters (*Slc2a1* and *Slc2a3*) at 6 weeks of outlet obstruction. The mRNA level of *Ldha* was increased, but *Pdk1*, which together with *Ldha* inhibits pyruvate from entering the citric acid cycle in mitochondria, was unchanged. Additional HIF targets, including *Lox*, *Edn1*, *Met* and *Pim1*, were also increased at 6 weeks (Figure 3b). Time-courses for these HIF target mRNAs, including *P4ha1*, which all exhibited significant elevations ($q=0$) at 10 days, are shown in Supplementary Figure 1.

HIF target protein levels were measured using western blotting, and in many cases (Figure 3c) a progressive rise from a low level in sham-operated controls to a higher level at 6 weeks was seen (summarized data in Figure 3d). The most marked increases were seen for Pim1, Edn1 (preproendothelin-1) and Ldha. Pim1 was largely undetectable in sham-operated rats but a pronounced band was seen at 6 weeks (Figure 3c). Pgk1 was not significantly increased (Figure 3d), representing one of few examples of a discrepancy between protein and mRNA data. Importantly, both glucose transporters and glycolytic enzymes were increased (Figure 3d).

HIF Target Gene Expression in Detrusor Smooth Muscle

Detrusor muscle contributes the largest relative fraction of the wet weight of the bladder, but the mucosal layer also contributes. To determine if the HIF target expression increases

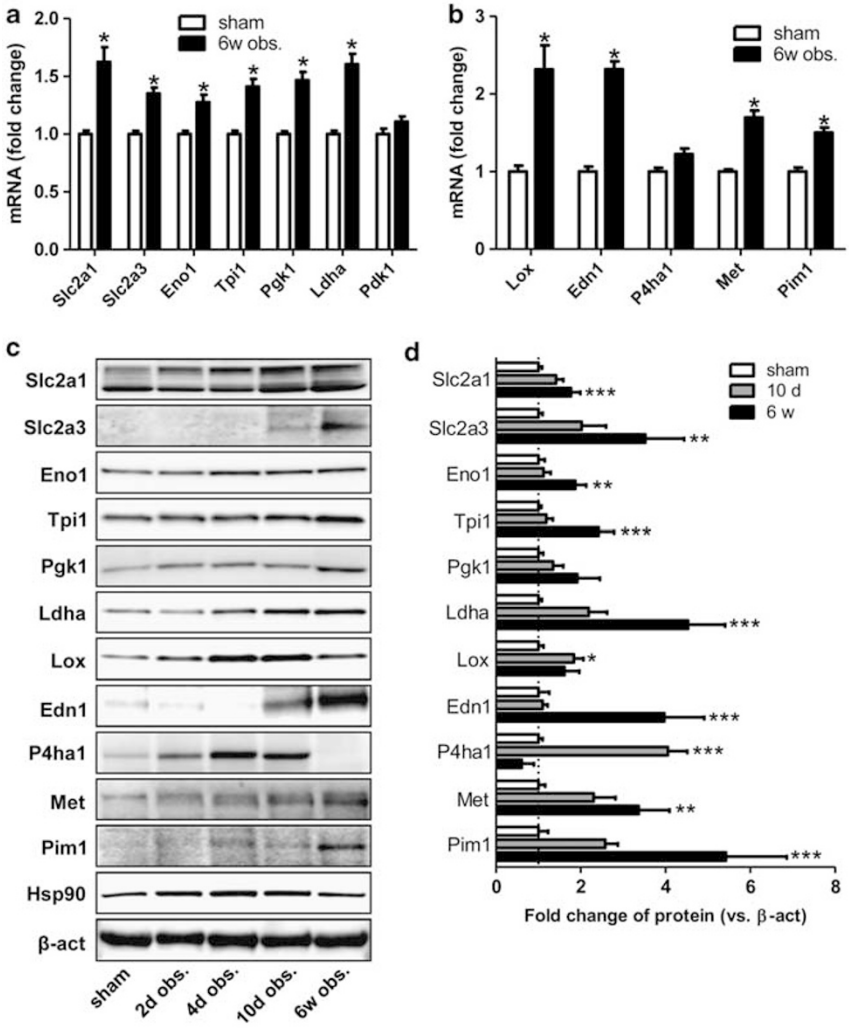

Figure 3 Glucose transporters, glycolytic enzymes and other HIF-1 signature targets are increased in bladder outlet obstruction. Panels **a** and **b** show mRNA levels in sham-operated control bladders (white bars) and in bladders obstructed for 6 weeks (black bars). Metabolic enzymes and transporters are grouped in panel **a**. The data are from a microarray experiment.[22] *Indicates $q = 0$. Panel **c** shows western blots for all the HIF-1 signature targets in panels **a** and **b**. Hsp90 and β-actin were used as loading controls. Panel **d** shows summarized data from the experiments in panel **c**. $n = 6$–8 throughout. *$P < 0.05$, **$P < 0.01$ and ***$P < 0.001$.

in smooth muscle, we used immunofluorescence staining. We observed a clear-cut increase of Edn1 in the detrusor smooth muscle cells of obstructed rats (green staining in top panels of Figure 4). Caveolin-1 staining (red) was used to trace the outline of individual cells, showing the characteristic non-continuous membrane staining. The HIF target *Slc2a1* (Glut-1, in green), a classical indicator of hypoxia and HIF activity, similarly increased in smooth muscle at 6 weeks of obstruction (compare c and d in Figure 4). Slc2a1 staining was membrane-associated in sham (arrows in c) but appeared to be primarily cytoplasmic in specimens from obstructed rats.

Bladder Outlet Obstruction and Mitophagy

HIF is considered to inhibit mitochondrial biogenesis in part through transcriptional upregulation of *Mxi1* and repression of *Ppargc1b*.[9] *Mxi1* tended to increase at 6 weeks, but this did not quite reach the level of statistical significance (Figure 5a). *Ppargc1b*, on the other hand, was reduced at 10 days (Figure 5a), preceding *Mxi1* upregulation. This suggested some other mechanism of *Ppargc1b* repression. No changes in nuclear respiratory factors, downstream mediators of *Ppargc1b* in mitochondrial biogenesis, were seen (data not shown). In view of this complexity, we focused instead on mitochondrial elimination. HIF-mediated removal of mitochondria occurs through Bnip3-mediated autophagy. *Bnip3* was elevated at the mRNA (Figure 5b) and protein levels (Figure 5c, top blot) at 6 weeks of obstruction. The mRNA level remained high following de-obstruction (Figure 5b). We therefore measured LC3B, a widely used indicator of the autophagic process. LC3B (*Map1lc3b*) increased slightly but

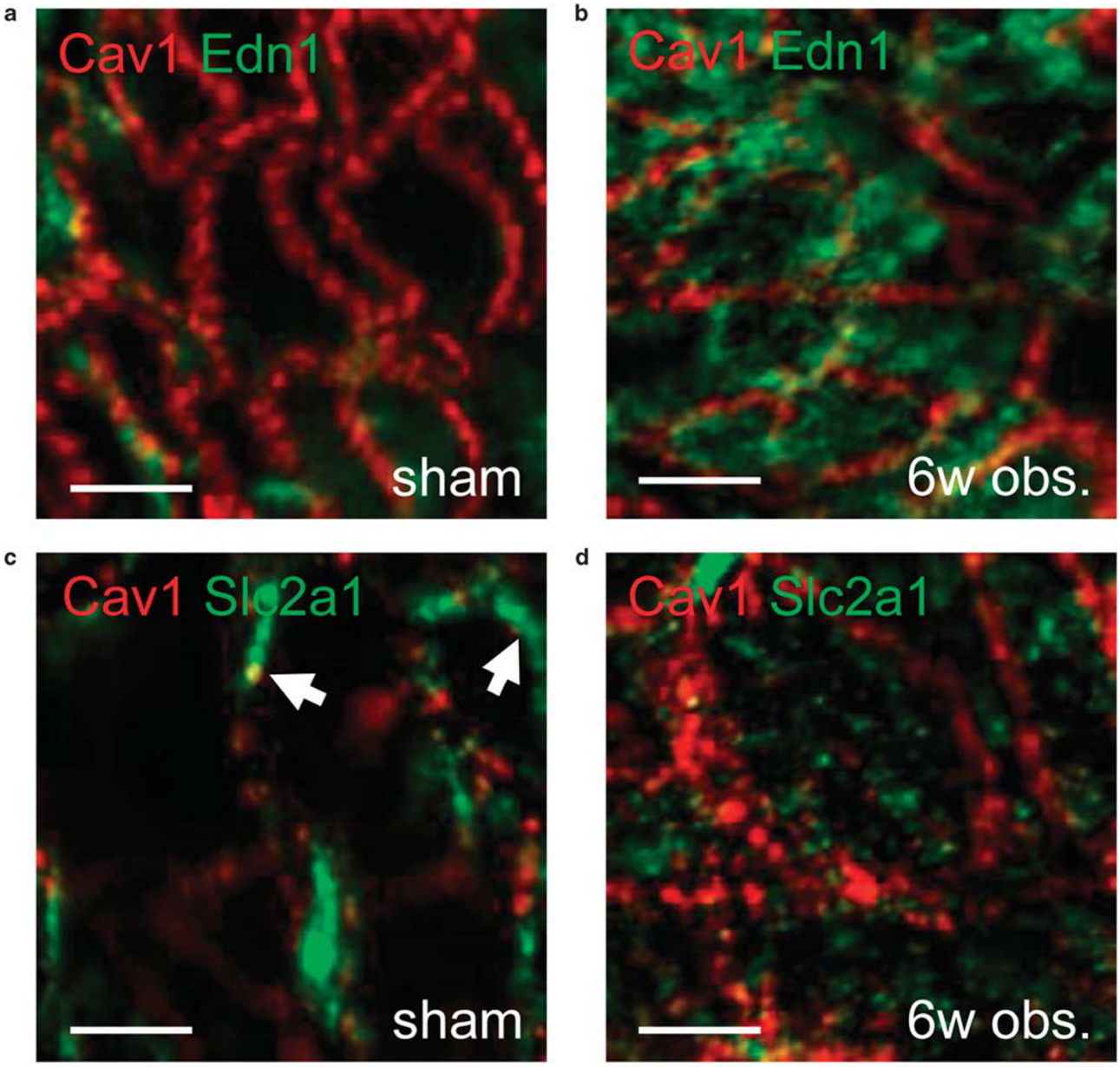

Figure 4 Increased staining for preproendothelin-1 (Edn1) and Glut-1 (Slc2a1) in detrusor smooth muscle at 6 weeks of obstruction. Edn1 (**a**, **b**) and Slc2a1 (**c**, **d**) (both in green) were examined using immunofluorescence in sham-operated (**a**, **c**) and obstructed bladders (6 weeks, **b**, **d**). Caveolin-1 staining (red) was used to distinguish the membrane. Approximately 15 cross-sectioned cell profiles are seen in panel **a**. Note that Caveolin-1 staining of the membrane is discontinuous reflecting the non-overlapping domain organization (caveolar domains: red, dense bands: black) of the smooth muscle cell plasmalemma. The arrows in panel **c** point to membrane-associated (membrane-near) staining for Slc2a1. Scale bars represent 5 μm.

not significantly at the mRNA level (Figure 5b), and yet total LC3B was clearly increased at the protein level at 6 weeks of obstruction (Figure 5c, middle blot). Summarized data showed that the processed form, LC3B-II, was significantly increased relative to β-actin (Figure 5d).

We next used electron microscopy to determine mitochondrial mass and to search for autophagosomes containing mitochondria. Figures 6a and b show examples of detrusor smooth muscle cells from a sham-operated and an obstructed (6 weeks) rat, respectively. We observed occasional autophagosome-like structures (Figure 6c), but they were present both in obstructed bladders and in controls. The number of mitochondria (Figure 6d), their minor diameter (Figure 6e) and their relative area (Figure 6f) was unchanged. We therefore measured mitochondrial markers by western blotting. Suox (sulfite oxidase) was transiently reduced (Figure 6g and summarized data in 6h). Ndufaf1 (an assembly factor for the NADH dehydrogenase subcomplex) and Cs (citrate

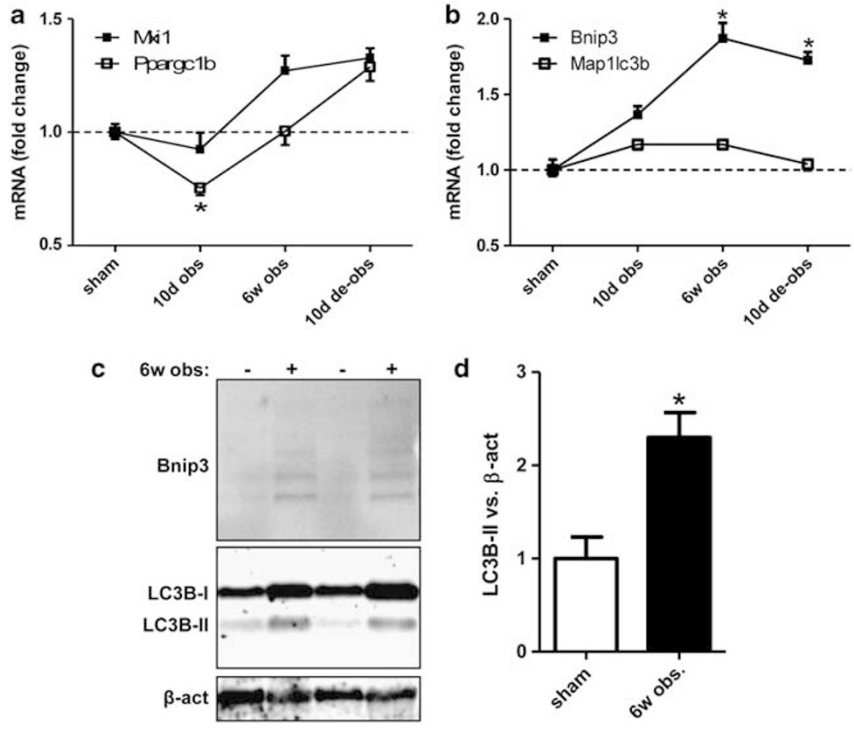

Figure 5 Biochemical support for mitophagy in bladder outlet obstruction. Panels **a** and **b** show mRNA levels for effectors of mitochondrial biogenesis (**a**) and mitochondrial removal by autophagy (**b**). Data are from microarrays run using sham-operated rats, rats obstructed for 10 days and 6 weeks, respectively, and from rats obstructed and re-operated at 6 weeks to remove the obstruction. Panel **c** shows western blots for the autophagy receptor Bnip3 and its ligand LC3B. Following synthesis, the C-terminus of LC3B is cleaved to produce LC3B-I, which is then modified by phosphatidylethanolamine to give LC3B-II, a marker of autophagy. Summarized data on LC3B-II normalized to β-actin are shown in panel **d**. $n = 4$–8 throughout. In panels **a** and **b** * denotes $q = 0$. In panel **d** * denotes $P < 0.05$.

synthase) were largely unchanged (Figure 6g). Total Cox4 (cytochrome *c* oxidase subunit IV), on the other hand was elevated fourfold at 6 weeks (Figure 6g and summarized data in 6i). We also measured the mitochondrial transcription factor Tfam (Figures 6g and j) and found that it was elevated at 6 weeks.

Metabolic Switching Confers Resistance to Mitochondrial Inhibition

HIF-mediated metabolic switching should result in reduced dependence on mitochondrial energy production and a greater dependence on energy production from glycolysis. As a major energetic cost is incurred by contraction and emptying of the bladder, we measured sensitivity of contraction to the mitochondrial inhibitor cyanide. As predicted, reduced relaxation by cyanide was observed after 6 weeks of obstruction compared with sham (Figure 7a, summarized data in Figure 7b). We next addressed whether a similar effect was provoked when HIF was activated during organ culture of detrusor muscle strips using DMOG. This substance causes HIF induction via molecular mechanisms that are distinct from hypoxia and, as expected, DMOG caused upregulation of the HIF targets Ldha and P4ha1 in cultured detrusor strips (Figure 7c, summarized data in 7d and e). DMOG moreover counteracted relaxation by cyanide (Figure 7f and summarized data in 7g).

DISCUSSION

Our study extends knowledge regarding the molecular processes that underlie metabolic adaptation in the urinary bladder following outlet obstruction. Previous work demonstrated increased bladder lactate production in outlet obstruction[21] and reduced bladder O_2 consumption,[20] but those findings were not put in context of the full program of metabolic changes now known to be orchestrated by HIF.[5] Here we demonstrate that outlet obstruction remodels mitochondria in the bladder, and we demonstrate increased expression of glucose transporters and glycolytic enzymes which, together with increased expression of lactate dehydrogenase (*Ldha*), is expected to redirect glucose metabolism toward production of lactate. We also demonstrate that the metabolic changes in the bladder confer a greater resistance of contraction to acute mitochondrial inhibition. Several of the individual genes that we studied are regulated by other factors than HIF, but no other factor comprehensively regulates transcription of all of these genes. Indeed, we found that functional and expressional changes caused by

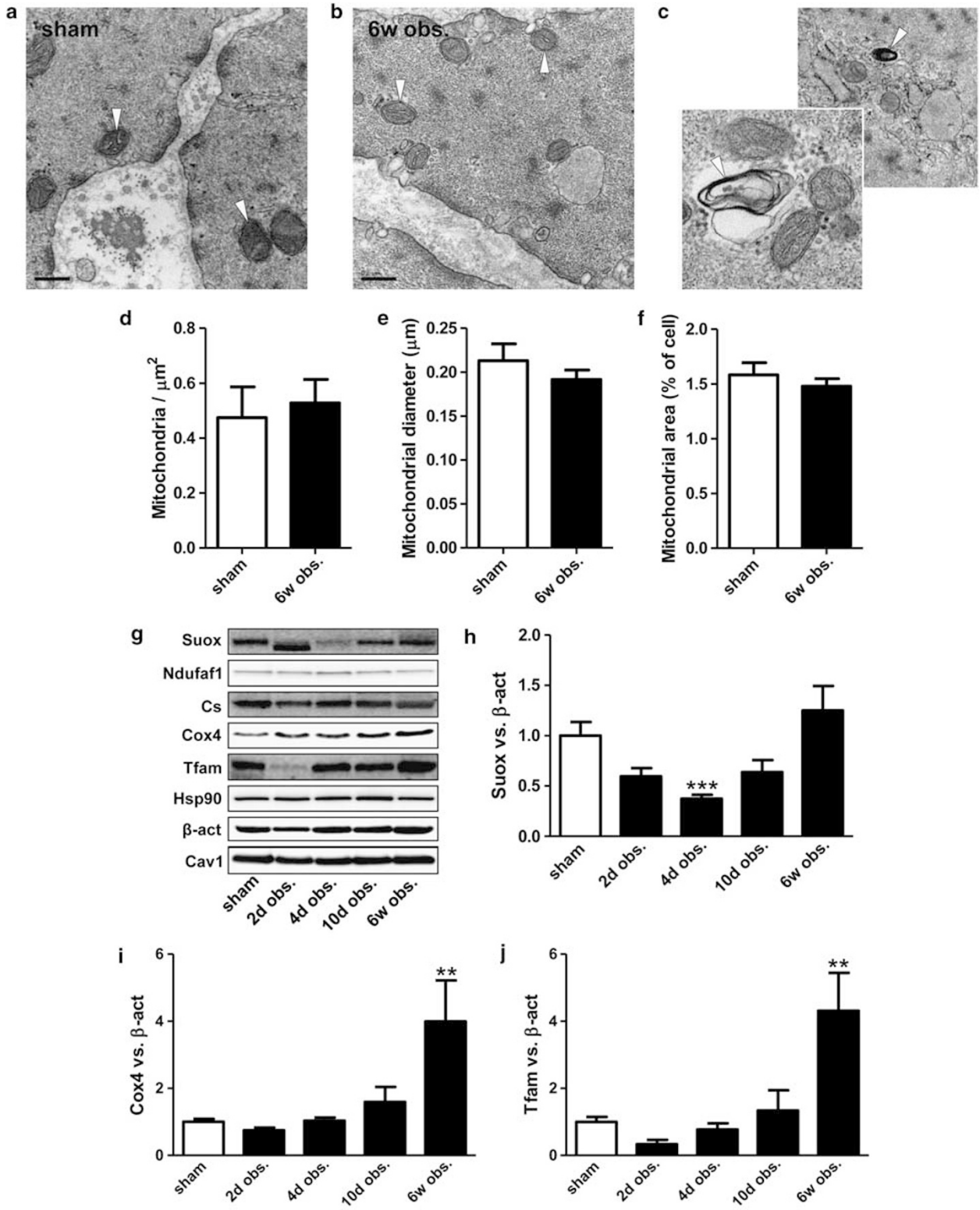

Figure 6 Maintained mitochondrial mass in outlet obstruction but remodeling of the mitochondrial proteome. Mitochondria in detrusor smooth muscle were measured using electron microscopy. Panels **a** and **b** show examples of smooth muscle cells from control and obstructed (6 weeks) bladders, respectively. Typical mitochondria are indicated with white arrowheads. Panel **c** demonstrates two examples of putative autophagosomes (arrowheads), which were rare and present both in control and obstructed bladders. Panels **d** through **f** show summaries of mitochondrial numbers, size, and area in control and obstructed bladders ($n=3$). Panel **g** shows western blots for four mitochondrial markers, Tfam and three loading controls (Hsp90, β-actin, caveolin-1). Panels **h** through **j** show quantitative summaries of the western blots in panel **g** ($n=6$). Bar graph summaries for Ndufaf1 and Cs were omitted as no significant differences were seen. ** and *** denote $P<0.01$ and $P<0.001$, respectively.

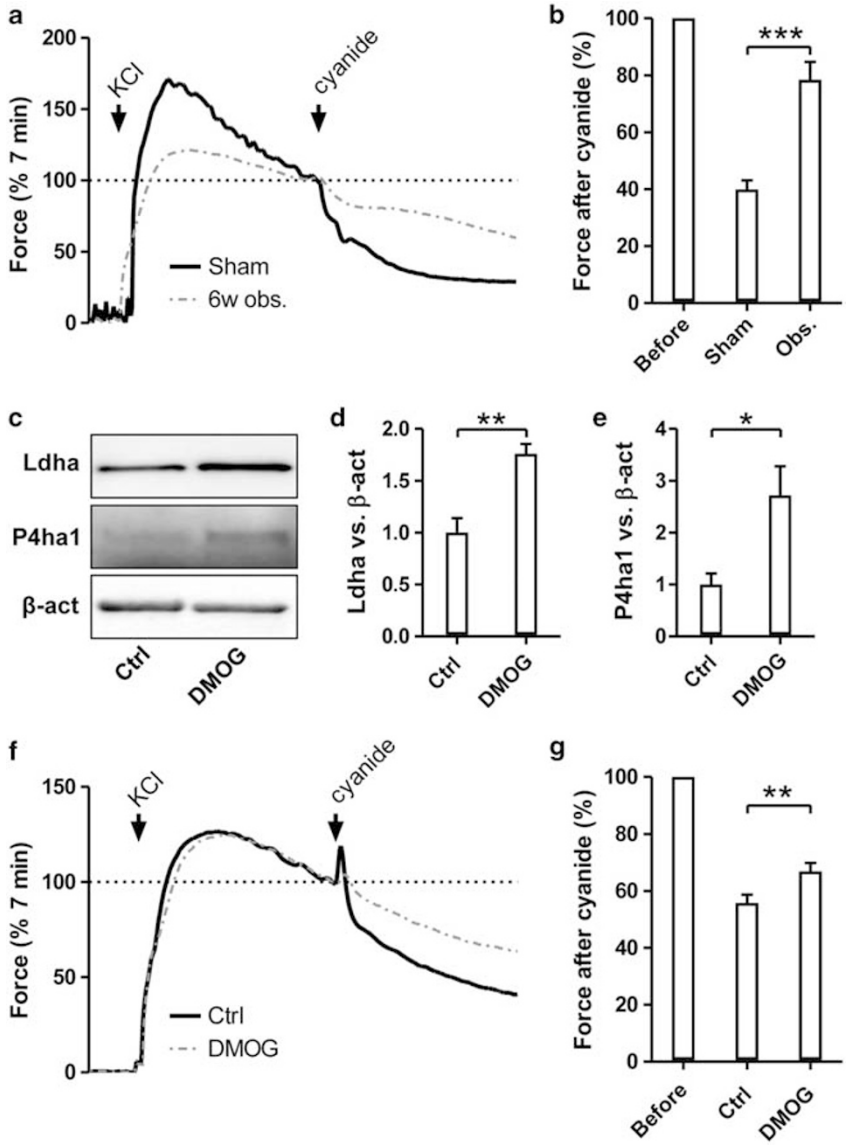

Figure 7 Bladder outlet obstruction confers resistance to mitochondrial inhibition. Detrusor strips were prepared from sham-operated and obstructed bladders and mounted in a myograph. Panel **a** shows the force in response to stimulation with KCl (60 mM) and subsequent relaxation by the mitochondrial inhibitor cyanide. Traces were normalized to the force level just before addition of cyanide. Panel **b** shows compiled data from the experiment in panel **a**. Panel **c** shows western blots for Ldha, P4ha1 and β-actin in strips cultured for 5 days in the absence (Ctrl) and presence of the HIF-inducer dimethyloxalylglycine (DMOG). Quantification of Ldha and P4ha1 expression is shown in the bar graphs in panels **d** and **e**. Panels **f** and **g** show force traces and summarized mechanical data from bladder strips maintained in organ culture with and without DMOG. $n = 4$ throughout. $^{*}P < 0.05$, $^{**}P < 0.01$ and $^{***}P < 0.001$.

obstruction are mimicked by pharmacological activation of HIF.

An unexpected outcome of our experiments was that HIF target mRNAs increased before a significant accumulation of HIF-1α protein was detected. A number of earlier reports have measured HIF-1α protein accumulation in the bladder in response to partial bladder outlet obstruction. Using western blotting, Ghafar *et al*[1] found accumulation of HIF-1α protein within 24 h of outlet obstruction, rising progressively throughout 14 days. Rats were used similar to our study, but the sample was small ($n = 2$). Matsumoto *et al*[25] found HIF-1α to be increased at 20 weeks using western blotting. Those experiments were done in the presence of a chemical carcinogen and no earlier times were investigated. Another study demonstrated HIF-1 activation at 2 weeks,[26] and because a gel shift assay was used, the outcome is fully compatible with an alternative mechanism of HIF activation. HIF-1α accumulation has also been studied using immunohistochemistry. Koritsiadis *et al*[2] convincingly demonstrated HIF-1α accumulation in the human bladder at a mean obstruction duration of 6 years. Another study in mice demonstrated HIF-1α accumulation in the detrusor at 4 weeks

of obstruction.[27] A number of studies have also documented increased HIF-1α mRNA in outlet obstruction, but the mRNA level, arguably, only has indirect bearing on HIF-1-mediated transcriptional activation. Therefore, to the best of our knowledge, only one prior study, with rather limited power,[1] challenges our present finding that HIF-mediated transcriptional activation precedes HIF-1α protein accumulation in outlet obstruction.

We were at first reticent to rule out HIF-1α protein accumulation at 10 days when HIF target mRNAs were clearly increased. We therefore used two different HIF-1α antibodies to ascertain that the band we studied actually represents HIF-1α. One of the series of lysates used for western blotting was moreover from the same bladders that were used for the TFBS analysis (10 days and 6 weeks). The conclusion that HIF-1α accumulation is a late event in our obstruction model, occurring after transcription of HIF target genes, is therefore unavoidable.

Our experiments demonstrate induction of HIF-2α at 10 days, preceding HIF-1α accumulation. This seems to agree with the differential oxygen sensitivities of the two isoforms. HIF-2α is activated by moderate hypoxia (5% O_2) whereas HIF-1α requires pronounced hypoxia (1% O_2).[28] Considerable target overlap for HIF-1α and HIF-2α exists, but certain genes are preferentially targeted by either factor.[29] Among the genes that are preferentially regulated by HIF-1α are *Ldha* and *Bnip3*.[30] As shown in Figure 5b and in Supplementary Figure 1b, these mRNAs peaked, or had at least started to increase, at 10 days when the HIF-1α protein remained at the level of sham-operated controls. It is therefore presently unclear if HIF-2α constitutes a sufficient explanation for the transcriptional activation at 10 days. Increased expression of *Arnt2* mRNA was previously reported and suggested to promote HIF-1 activation in bladder outlet obstruction.[17] Here we found that *Arnt2* (HIF-2β) and *Arntl2*, both of which are capable of forming transactivation competent heterodimers with HIF-1α,[16,18] are upregulated at the mRNA level in outlet obstruction already at 10 days. *Ahrr*, which encodes a protein that represses HIF-1α,[19] was reduced. Together, these changes may facilitate HIF-1 activation independently of HIF-1α protein accumulation in bladder outlet obstruction. The correlation between *Arnt2* and *Slc2a1* supports this possibility.

Apart from a HIF-driven switch in metabolism, we also document changes in enzymes of relevance for fibrosis (Lox and P4ha1) and signaling (Met, Pim1 and Edn1). In recent work, we showed that repression of miR-29 has a role in remodeling of the extracellular matrix following outlet obstruction.[22] Our current findings imply important synergies between hypoxia and miR-29, where repression of miR-29 is responsible in part for increased synthesis of elastin and collagen and where HIF, via Lox and P4ha1, is responsible for increased processing and cross-linking of these matrix proteins.

To more directly pinpoint the bladder compartment in which HIF-driven transcriptional activation occurs, we used immunofluorescence staining. We selected *Slc2a1* (Glut-1) and *Edn1* (endothelin-1) because the dynamic range of change was large for both. We examined the distribution of these antigens at 6 weeks and found that the staining of the detrusor layer was increased in comparison with sham-operated controls. Hypoxiprobe adducts were previously demonstrated in smooth muscle bundles in chronic obstruction[20] in good agreement with our current findings. Taken together, this implies an expressional impact of HIF in detrusor smooth muscle.

A theme that has recently emerged is that the HIF complex controls the number of mitochondria by opposing influences on mitochondrial biogenesis and removal; biogenesis is impaired and removal stimulated.[9,10] We focused our effort on the possibility that HIF causes mitophagy. We found that Bnip3, a transmembrane protein localized to mitochondria and that binds to LC3B-II on the phagophore,[31] was increased at the protein level at 6 weeks. We moreover found a doubling of LC3B-II. However, using electron microscopy, we found that autophagic organelles containing mitochondria were very rare and that the mitochondrial size and area were unchanged. Together, these findings imply either that mitophagy occurs elsewhere in the bladder, or that autophagosomes are undetectable by electron microscopy due, for example, to a short lifespan. If the latter possibility is correct, the expected HIF-mediated reduction of mitochondrial mass must be overridden by some other influence. This possibility is supported by our finding that Tfam, a transcription factor that controls mitochondrial mass,[32] was elevated at 6 weeks.

One mechanism by which HIF optimizes mitochondrial respiration is by switching of the cytochrome *c* oxidase isoform from Cox4-1 to Cox4-2.[12] This increases the efficiency of respiration in hypoxia. In some cells, such as Hep3b cells and smooth muscle cells, this response is dominated by an increased expression of Cox4-2 with little repression of Cox4-1.[12] Consistent with this paradigm, our blots using an antibody that detects total Cox4, showed a progressive increase in Cox4 expression. Three other mitochondrial markers (Suox, Ndufaf1 and Cs) were unchanged or transiently reduced, suggesting specific targeting of Cox4 compared with other mitochondrial proteins. Together, these observations support the view that bladder outlet obstruction is associated with remodeling of the mitochondrial proteome.

A normal micturition cycle is critical for maintained kidney function. In a situation when the outlet resistance is increased, the bladder must contract more forcefully and generate a higher pressure over a longer time to overcome the resistance. This is expected to cause more pronounced ischemia. Metabolic adaptation (switching) that allows the bladder to contract forcefully in oxygen-limited conditions would help maintain a normal micturition cycle. Here we demonstrate that obstructed bladders are less sensitive to mitochondrial inhibition and that this effect is mimicked by HIF activation using DMOG independent of outlet obstruction. This is well in line with older work showing reduced sensitivity of the obstructed bladder to hypoxia.[33,34]

Therefore, HIF-driven metabolic adaptation likely allows for effective emptying of the obstructed urinary bladder.

Taken together, our findings argue that HIF activation in outlet obstruction involves mechanisms beyond the accumulation of HIF-1α protein. We directly demonstrate accumulation of HIF-2α and of Arnt2 together with repression of *Ahrr*. This may explain HIF activation without apparent HIF-1α accumulation early after obstruction. We moreover show that HIF activation in outlet obstruction is associated with increased expression of glucose transporters and glycolytic enzymes, together with remodeling of the mitochondrial proteome. These changes go hand in hand with a reduced sensitivity of contraction to mitochondrial inhibition. The metabolic switching orchestrated by HIF in obstructed bladders ensures maintained contractility in oxygen-limited conditions and thereby likely upholds a normal micturition cycle.

Supplementary Information accompanies the paper on the Laboratory Investigation website (http://www.laboratoryinvestigation.org)

ACKNOWLEDGMENTS

Work in the authors' laboratories is supported by the Swedish Research Council, the Greta and Johan Kock's Foundation, the Crafoord Foundation, the Medical Faculty at Lund University, the Royal Physiographic Society, Gösta Jonsson's foundation and regional health care grants. We thank Karolina Turczyńska for advice on organ culture and Ola Gustafsson for help with electron microscopy.

DISCLOSURE/CONFLICT OF INTEREST

The authors declare no conflict of interest.

1. Ghafar MA, Anastasiadis AG, Olsson LE, *et al.* Hypoxia and an angiogenic response in the partially obstructed rat bladder. Lab Invest 2002;82:903–909.
2. Koritsiadis G, Stravodimos K, Koutalellis G, *et al.* Immunohistochemical estimation of hypoxia in human obstructed bladder and correlation with clinical variables. BJU Int 2008;102:328–332.
3. Buttyan R, Chichester P, Stisser B, *et al.* Acute intravesical infusion of a cobalt solution stimulates a hypoxia response, growth and angiogenesis in the rat bladder. J Urol 2003;169:2402–2406.
4. Pugh CW, Ratcliffe PJ. Regulation of angiogenesis by hypoxia: role of the HIF system. Nat Med 2003;9:677–684.
5. Semenza GL. Hypoxia-inducible factors in physiology and medicine. Cell 2012;148:399–408.
6. Jaakkola P, Mole DR, Tian YM, *et al.* Targeting of HIF-alpha to the von Hippel-Lindau ubiquitylation complex by O2-regulated prolyl hydroxylation. Science 2001;292:468–472.
7. Schodel J, Oikonomopoulos S, Ragoussis J, *et al.* High-resolution genome-wide mapping of HIF-binding sites by ChIP-seq. Blood 2011; 117:e207–e217.
8. Semenza GL, Roth PH, Fang HM, *et al.* Transcriptional regulation of genes encoding glycolytic enzymes by hypoxia-inducible factor 1. J Biol Chem 1994;269:23757–23763.
9. Zhang H, Gao P, Fukuda R, *et al.* HIF-1 inhibits mitochondrial biogenesis and cellular respiration in VHL-deficient renal cell carcinoma by repression of C-MYC activity. Cancer Cell 2007;11:407–420.
10. Zhang H, Bosch-Marce M, Shimoda LA, *et al.* Mitochondrial autophagy is an HIF-1-dependent adaptive metabolic response to hypoxia. J Biol Chem 2008;283:10892–10903.
11. Kim I, Rodriguez-Enriquez S, Lemasters JJ. Selective degradation of mitochondria by mitophagy. Arch Biochem Biophys 2007;462:245–253.
12. Fukuda R, Zhang H, Kim JW, *et al.* HIF-1 regulates cytochrome oxidase subunits to optimize efficiency of respiration in hypoxic cells. Cell 2007;129:111–122.
13. Keith B, Johnson RS, Simon MC. HIF1alpha and HIF2alpha: sibling rivalry in hypoxic tumour growth and progression. Nat Rev Cancer 2012;12:9–22.
14. Maltepe E, Keith B, Arsham AM, *et al.* The role of ARNT2 in tumor angiogenesis and the neural response to hypoxia. Biochem Biophys Res Commun 2000;273:231–238.
15. Sekine H, Mimura J, Yamamoto M, *et al.* Unique and overlapping transcriptional roles of arylhydrocarbon receptor nuclear translocator (Arnt) and Arnt2 in xenobiotic and hypoxic responses. J Biol Chem 2006;281:37507–37516.
16. Keith B, Adelman DM, Simon MC. Targeted mutation of the murine arylhydrocarbon receptor nuclear translocator 2 (Arnt2) gene reveals partial redundancy with Arnt. Proc Natl Acad Sci USA 2001;98: 6692–6697.
17. Stephany HA, Strand DW, Ching CB, *et al.* Chronic cyclic bladder over distention up-regulates hypoxia dependent pathways. J Urol 2013; 190:1603–1609.
18. Hogenesch JB, Gu YZ, Moran SM, *et al.* The basic helix-loop-helix-PAS protein MOP9 is a brain-specific heterodimeric partner of circadian and hypoxia factors. J Neurosci 2000;20:RC83.
19. Karchner SI, Jenny MJ, Tarrant AM, *et al.* The active form of human aryl hydrocarbon receptor (AHR) repressor lacks exon 8, and its Pro 185 and Ala 185 variants repress both AHR and hypoxia-inducible factor. Mol Cell Biol 2009;29:3465–3477.
20. Kato K, Lin AT, Haugaard N, *et al.* Effects of outlet obstruction on glucose metabolism of the rabbit urinary bladder. J Urol 1990;143: 844–847.
21. Polyanska M, Arner A, Malmquist U, *et al.* Lactate dehydrogenase activity and isoform distribution in the rat urinary bladder: effects of outlet obstruction and its removal. J Urol 1993;150:543–545.
22. Ekman M, Bhattachariya A, Dahan D, *et al.* Mir-29 repression in bladder outlet obstruction contributes to matrix remodeling and altered stiffness. PLoS.One 2013;8:e82308.
23. Veerla S, Ringner M, Hoglund M. Genome-wide transcription factor binding site/promoter databases for the analysis of gene sets and co-occurrence of transcription factor binding motifs. BMC Genomics 2010;11:145.
24. Gomez M, Sward K. Long-term regulation of contractility and calcium current in smooth muscle. Am J Physiol 1997;273:C1714–C1720.
25. Matsumoto S, Shimizu N, Hanai T, *et al.* Bladder outlet obstruction accelerates bladder carcinogenesis. BJU Int 2009;103:1436–1439.
26. McGonagle E, Smith A, Butler S, *et al.* Water avoidance stress results in an altered voiding phenotype in male mice. Neurourol Urodyn 2012;31:1185–1189.
27. Drzewiecki BA, Anumanthan G, Penn HA, *et al.* Modulation of the hypoxic response following partial bladder outlet obstruction. J Urol 2012;188:1549–1554.
28. Holmquist-Mengelbier L, Fredlund E, Lofstedt T, *et al.* Recruitment of HIF-1alpha and HIF-2alpha to common target genes is differentially regulated in neuroblastoma: HIF-2alpha promotes an aggressive phenotype. Cancer Cell 2006;10:413–423.
29. Hu CJ, Sataur A, Wang L, *et al.* The N-terminal transactivation domain confers target gene specificity of hypoxia-inducible factors HIF-1alpha and HIF-2alpha. Mol Biol Cell 2007;18:4528–4542.
30. Wang V, Davis DA, Haque M, *et al.* Differential gene up-regulation by hypoxia-inducible factor-1alpha and hypoxia-inducible factor-2alpha in HEK293T cells. Cancer Res 2005;65:3299–3306.
31. Hanna RA, Quinsay MN, Orogo AM, *et al.* Microtubule-associated protein 1 light chain 3 (LC3) interacts with Bnip3 protein to selectively remove endoplasmic reticulum and mitochondria via autophagy. J Biol Chem 2012;287:19094–19104.
32. Scarpulla RC. Transcriptional paradigms in mammalian mitochondrial biogenesis and function. Physiol Rev 2008;88:611–638.
33. Arner A, Malmqvist U, Uvelius B. Metabolism and force in hypertrophic smooth muscle from rat urinary bladder. Am J Physiol 1990;258: C923–C932.
34. Levin RM, English M, Barretto M, *et al.* Normal detrusor is more sensitive than hypertrophied detrusor to in vitro ischemia followed by re-oxygenation. Neurourol Urodyn 2000;19:701–712.